Acta Geophysica
https://doi.org/10.1007/s11600-017-0103-0

RESEARCH ARTICLE - APPLIED GEOPHYSICS

Comparison of SPT and V_s-based liquefaction analyses: a case study in Erciş (Van, Turkey)

İsmail Akkaya[1] · Ali Özvan[2] · Mutluhan Akin[3] · Müge K. Akin[4] · Uğur Övün[2]

Received: 4 June 2017 / Accepted: 1 December 2017

Abstract
Liquefaction which is one of the most destructive ground deformations occurs during an earthquake in saturated or partially saturated silty and sandy soils, which may cause serious damages such as settlement and tilting of structures due to shear strength loss of soils. Standard (SPT) and cone (CPT) penetration tests as well as the shear wave velocity (V_s)-based methods are commonly used for the determination of liquefaction potential. In this research, it was aimed to compare the SPT and V_s-based liquefaction analysis methods by generating different earthquake scenarios. Accordingly, the Erciş residential area, which was mostly affected by the 2011 Van earthquake ($M_w = 7.1$), was chosen as the model site. Erciş (Van, Turkey) and its surroundings settle on an alluvial plain which consists of silty and sandy layers with shallow groundwater level. Moreover, Çaldıran, Erciş–Kocapınar and Van Fault Zones are the major seismic sources of the region which have a significant potential of producing large magnitude earthquakes. After liquefaction assessments, the liquefaction potential in the western part of the region and in the coastal regions nearby the Lake Van is found to be higher than the other locations. Thus, it can be stated that the soil tightness and groundwater level dominantly control the liquefaction potential. In addition, the lateral spreading and sand boiling spots observed after the 23rd October 2011 Van earthquake overlap the scenario boundaries predicted in this study. Eventually, the use of V_s-based liquefaction analysis in collaboration with the SPT results is quite advantageous to assess the rate of liquefaction in a specific area.

Keywords Liquefaction · SPT · Shear wave velocity (V_s) · LPI · LSI · Erciş

Introduction

In addition to the structural quality, surface deformations (liquefaction, lateral spreading, etc.) which occur due to adverse soil properties, have a significant role in the loss of life and property during earthquakes. Liquefaction occurs as a result of earthquakes in loose sandy, silty soils and areas with shallow groundwater level. Pore water pressure between the soil particles increases due to earthquake waves during liquefaction. Once, the pore water pressure and the total stress are equal, the frictional force between the soil particles, in other words, the effective stress reaches to zero. Thus, bearing capacity and sudden settlement problems occur in the foundation ground and there may be significant structural problems such as overturning of structures. Liquefaction is mostly observed after moderate to high magnitude earthquakes. It is very important to determine the liquefaction potential of the ground under dynamic loads to prevent damage due to liquefaction.

Following the 1964 earthquake in Japan, lots of studies have been carried out to explain soil liquefaction. Shear wave velocity measurements, CPT and SPT, have been used by many researchers for determining the liquefaction potential of soils (Seed and Idriss 1971; Dobry et al. 1982; Iwasaki et al. 1982; Tokimatsu and Yoshimi 1983; Ishihara 1996; Kramer 1996; Robertson and Wride 1998; Juang et al. 2003; Cetin et al. 2004; Idriss and Boulanger

✉ İsmail Akkaya
iakkaya@yyu.edu.tr; iakkaya79@gmail.com

[1] Department of Geophysical Engineering, Engineering Faculty, Van Yüzüncü Yıl University, 65080 Van, Turkey

[2] Department of Geological Engineering, Van Yüzüncü Yıl University, Van, Turkey

[3] Department of Geological Engineering, Nevşehir Hacı Bektaş Veli University, Nevşehir, Turkey

[4] Department of Civil Engineering, Abdullah Gül University, Kayseri, Turkey

Published online: 08 December 2017

2006, 2008; Yi 2010). In addition, Andrus and Stokoe (2000), Uyanık (2002), Uyanik and Taktak (2009), Uyanik et al. (2013a) developed liquefaction analysis methods that depend upon the S wave velocity. Several empirical formulas were developed to determine the liquefaction potential using SPT-N values and V_s data using Seed and Idriss (1971) method (Dikmen 2009; Akın et al. 2011; Hasançebi and Ulusay 2007). V_s which is an important parameter used in earthquake engineering, is mainly used for determining the dynamic properties and liquefaction potential of soils (Karastathis et al. 2002; Soupios et al. 2005; Uyanık et al. 2006; Tezcan et al. 2006; Bozcu et al. 2007; Dadashpour et al. 2009; Uyanık and Ulugergerli 2008; Uyanik 2010, 2011; Uyanik et al. 2013b).

The SPT-N and V_s values are important physical parameters that may vary depending on porosity, effective stress, and relative density. V_s velocity is considered to be an easy and fast method as it can be applied both in the field and in the laboratory. In particular, liquefaction analysis based on V_s data, which can be easily obtained in environments where the SPT and CPT measurements cannot be performed, has been frequently used in recent years (Dobry et al. 1981b; Seed et al. 1983; Tokimatsu and Uchida 1990; Kayen et al. 1992; Andrus and Stokoe 2000; Uyanık 2002, 2006; Uyanik and Taktak 2009; Uyanik et al. 2013a; Duman and Ikizler 2014; Pekkan et al. 2015).

The liquefaction analysis methods based on SPT and laboratory data are frequently used. The studies in which liquefaction analysis methods based on SPT and V_s wave velocities coexist are limited.

In this study, Erciş (Van, Turkey) settlement area, which is under the effect of three different major fault zones, is selected as the study location. Erciş residential area is the largest district of the region located at the north of Lake Van, with more than 150,000 inhabitants (Fig. 1). A catastrophic earthquake of 7.1(M_w) shook the study area on 23rd October, 2011 at 13:41 local time (KOERI 2011). As a result of this earthquake, lateral spreading and liquefaction occured in the Erciş settlement area and in the close vicinity (Akın et al. 2013, 2015a, b; Aydan et al. 2012, 2013). The earthquake heavily damaged hundreds of buildings in Van and Erciş city, rendering them unusable. The Erciş settlement is classified in the first-degree seismic hazard zone of Turkey (ABYYHY 1997).

In this study, the grain size distribution of recent loose sediments and the presence of groundwater as well as the seismicity of the region were jointly investigated to determine the liquefaction potential of the subsurface soil. Liquefaction analysis was conducted using the V_s velocities and SPT-N values. Moreover, the advantages and disadvantages of these methods were highlighted by performing liquefaction analyses using both SPT and V_s data in a model area. Four different methodologies (SPT-based LPI and LSI, V_s-based threshold acceleration and safety factor) used for the assessment of liquefaction potential were taken into consideration. Moreover, the results of both methods were compared. Additionally, the liquefaction potential of the study area was determined on the basis of different magnitude earthquakes using the seismic data complied from 21 different sites along with the SPT values collected from a total of 165 different boreholes (Fig. 1). Finally, maps presenting the liquefaction potential were prepared and the results of the analyses were discussed. Different earthquake scenarios for three different active faults that can produce large earthquakes in the selected area were considered in these analyses.

Geology of the study area

The Lake Van basin, involving the Erciş settlement, consists of Late Cretaceous ophiolites and Tertiary marine sediments (Fig. 2a). A number of dissimilar rock masses and alluvium are traced in some locations of the Lake Van as shown in the geological map illustrated in Fig. 2b.

The Erciş province and its surroundings consist of three main geological units which are the basement rocks of the Erciş region. The limestone unit which is also known as the Lower Miocene aged Adilcevaz limestone, Pliocene–Pleistocene aged volcanics and volcano-sedimentary clasts and Quaternary–Holocene aged recent, and old alluviums and old lake sediments are the major geological units in the study area (Fig. 2). Volcanism occurred in various stages from Pliocene to Quaternary with different volcanic units in the region (Özdemir et al. 2006, 2016; Özdemir and Güleç 2014; Oyan et al. 2016). Erciş settlement is covered by old alluvial deposits of Quaternary age and the recent alluvium around Zilan Creek with Holocene age. This unit is comprised of loose and soft clay, sand, silt and gravels.

The groundwater level is shallow particularly around the Lake Van considering the borehole data (Fig. 3). While the groundwater level in the study area is generally observed after 5 m in old lake sediments, it is shallower than 5 m in the coastal sections of Lake Van and around Zilan Creek in recent alluvial deposits (Özvan et al. 2008; Akın et al. 2015a, b) (Fig. 3).

Seismic characteristics of the region

Erciş and its surroundings is located in the Lake Van basin at the Eastern Anatolian Plateau, that was formed due to the collision of Arabian and Eurasian Plates in Late Miocene (Şengör and Yılmaz 1981; Şengör and Kidd 1979; Koçyiğit et al. 2001). Attributable to these crustal movements, north–south direction compression in the region,

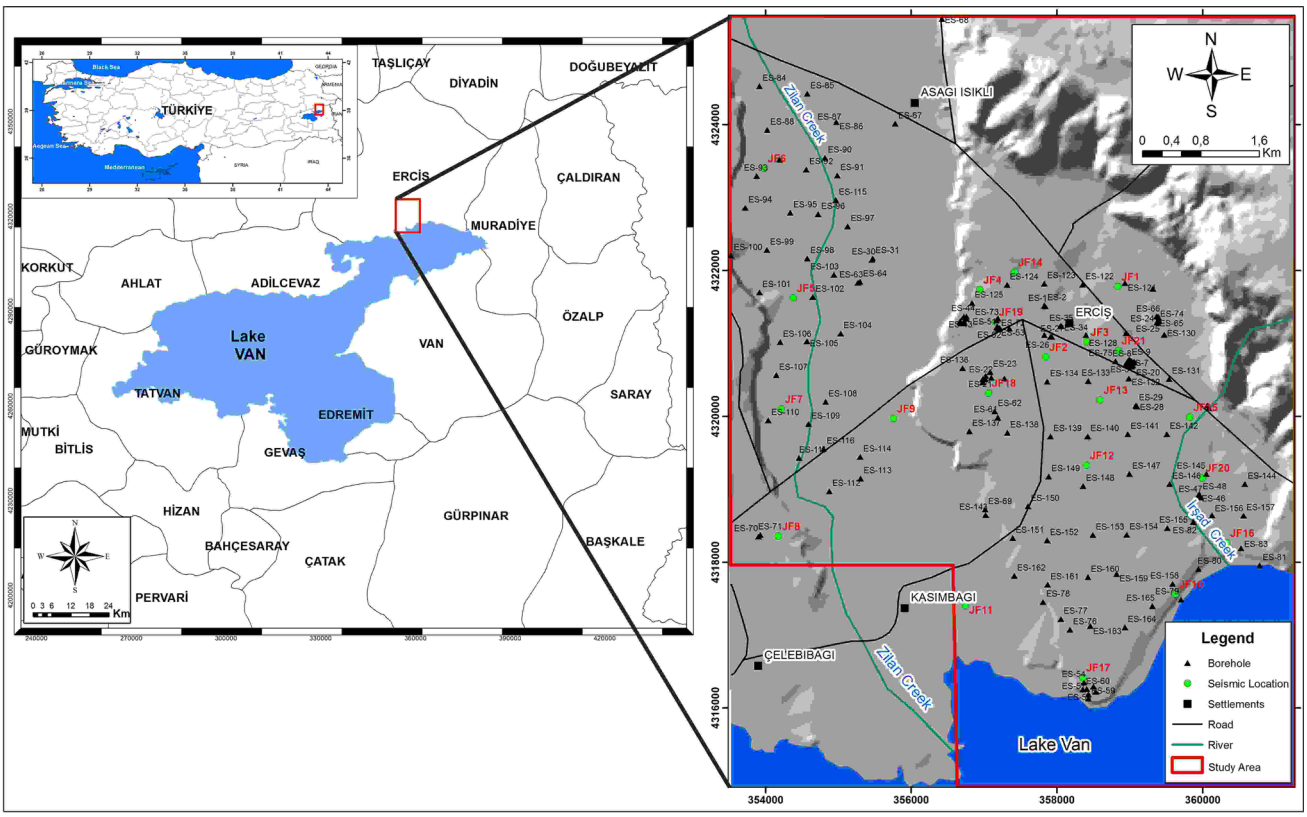

Fig. 1 Location map of the study area

east–west trending reverse faults and main folding axis and northeast–southwest left-lateral and northwest–southeast right-lateral strike-slip faults and north–south trending normal faults were developed (Şaroğlu and Yılmaz 1986; Koçyiğit et al. 2001; Bozkurt 2001; Koçyiğit 2013). The activity of all these tectonic structures supports the ongoing seismic activity in the region (Fig. 4, Table 1).

The Lake Van basin and its surrounding area has a very complex seismotectonic setting and active fault zones, such as Çaldiran fault zone, Çolpan fault, Erciş–Kocapınar fault zone, Süphan fault, Everek fault, Alaköy fault, Özalp fault, Gürpınar fault zone and Van thrust fault (Koçyiğit 2013; Selçuk 2016) (Fig. 4). Numerous devastating earthquakes have been documented around the Lake Van basin in the last century, such as 1941 Erciş ($M_s = 5.9$); 1945 Van ($M_s = 5.8$); 1966 Varto ($M_s = 6.8$); 1903 Malazgirt ($M_s = 6.3$); 1976 Çaldıran ($M_s = 7.3$); 2011 Van ($M_w = 7.1$) and 2011 Van ($M_w = 5.6$) earthquakes (Ambraseys 2001; Koçyiğit 2013). Erciş–Kocapınar Fault, Çaldıran Fault and Van Fault are important fault zones that can adversely affect the study area.

Liquefaction analyses

In the study area, liquefaction analyses were carried out according to different liquefaction analysis methods as well as dissimilar magnitude and acceleration values that can be produced by three different active faults. Experimental data of 165 boreholes drilled in the study area were used to evaluate Liquefaction Potential (LPI) and Liquefaction Severity (LSI) Index (Table 2). LPI (Iwasaki et al. 1982) and LSI (Sonmez and Gokceoglu 2005) values were calculated using the liquefaction safety factor of every geotechnical borehole. Idriss and Boulanger (2008) method, which depends on the ratio between cyclic stress ratio (CSR) and cyclic resistance ratio (CRR), was utilized for the determination of safety factor against liquefaction.

It is inevitable to use V_s as a parameter for the determination of liquefaction resistance. In this sense, seismic surface wave measurements (MASW) were performed at 21 points in the study area (Table 3). In this study, liquefaction analyses based on calculated V_s values and geotechnical data were performed.

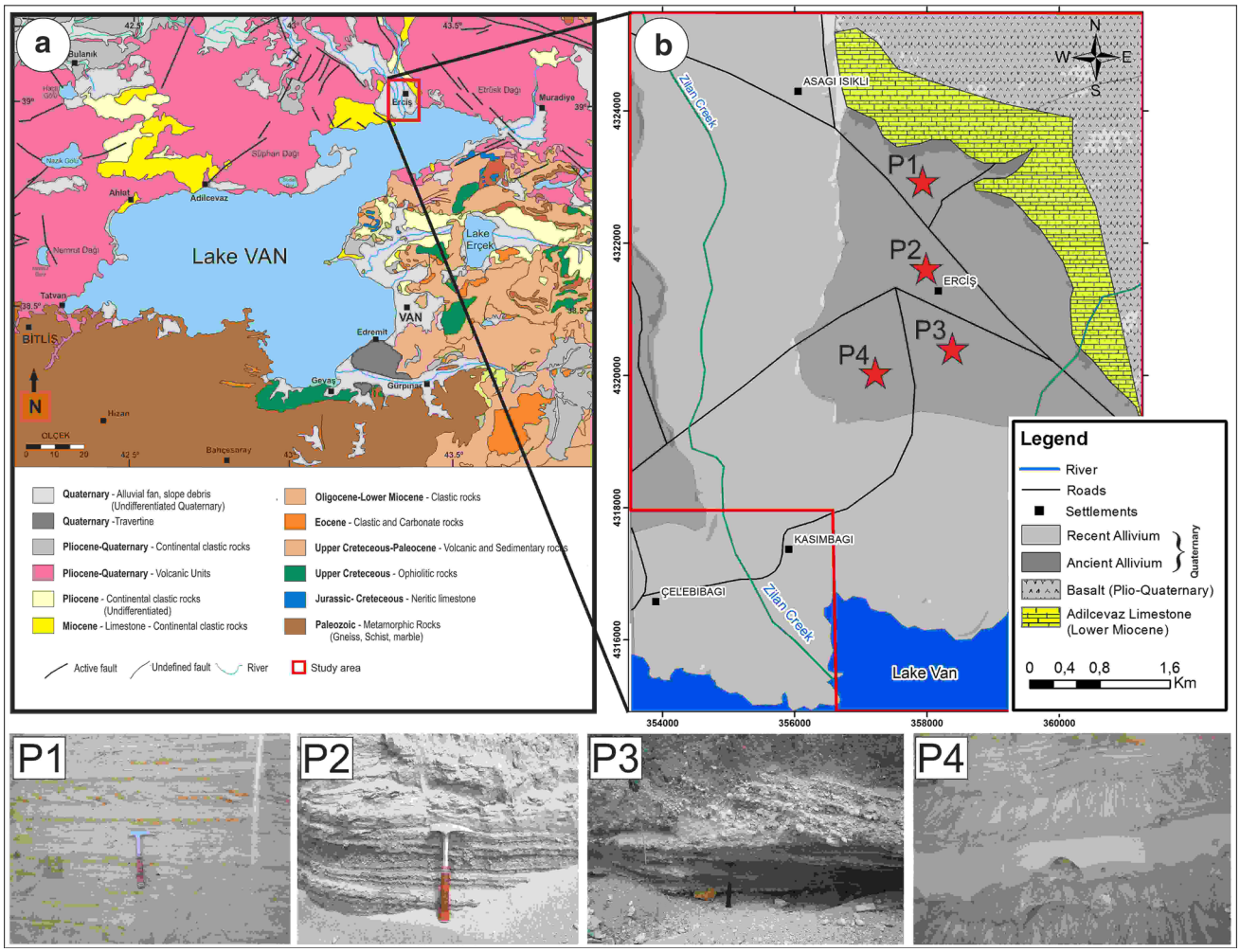

Fig. 2 The general geological map of Lake Van basin (modified from MTA, 2007) (**a**), geological map of Erciş (**b**) (Picture 1, 2, 3 and 4 refers to Quaternary aged alluvium units)

Calculated LPI, LSI, V_{s30} distribution, liquefaction potential according to threshold acceleration criteria, and safety factor liquefaction potential maps obtained according to V_s velocities were prepared using ArcMap10 Geographic Information Systems software. Inverse Distance Weighting (IDW) statistical method was utilized during the preparation of the maps. IDW interpolation designates cell values using weighted combination of sample points (Watson and Philip 1985).

Attenuation relationship for the determination of peak ground acceleration (a_{max})

In this study, scenario earthquakes were initially designed, and then liquefaction analyses were performed. Equations of liquefaction analyses are highly dependent on the peak ground acceleration (a_{max}) which is an important parameter for the scenario earthquakes.

In the liquefaction analyses based on SPT and V_s, active faults that may affect and/or affected the Erciş settlement area and the largest earthquakes that occurred in the region were considered. As a result of these analyses, magnitude (M), distance (R) and acceleration calculations were performed for three different active faults (Erciş–Kocapınar, Çaldıran and Van fault) that can adversely affect the study area (Table 4, Fig. 5). Major earthquakes that hit the region were gathered from the Kandilli Observatory and Earthquake Research Institute (KOERI) earthquake data. Each earthquake was expressed in terms of M_w using the magnitude conversion relations suggested by Kadirioğlu and Kartal (2016) after determining the largest earthquakes that occurred on three active faults (Table 4). Kadirioğlu and Kartal (2016) proposed M_S to M_w conversion as follows;

$$\begin{aligned} M_w &= 0.5716\,(\pm 0.024927)\,M_s \\ &\quad + 2.4980\,(\pm 0.117197) \qquad 3.4 \le M_s \le 5.4 \\ M_w &= 0.8126\,(\pm 0.034602)\,M_s \\ &\quad + 1.1723\,(\pm 0.208173) \qquad M_s \ge 5.5. \end{aligned} \tag{1}$$

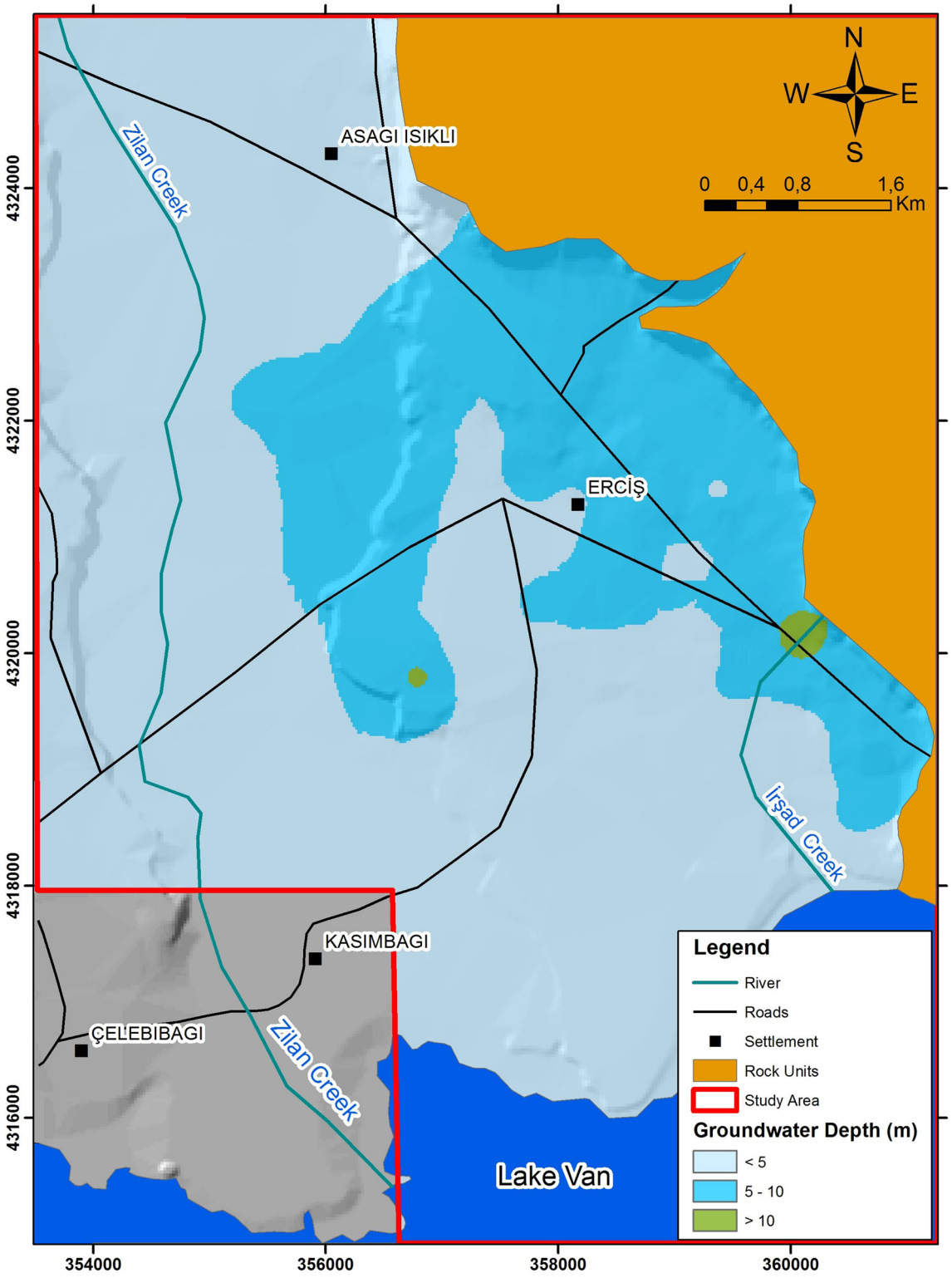

Fig. 3 Depth to groundwater level map of the study area

Using the magnitude and distance parameters obtained from the analyses, accelerations were calculated with the ground motion prediction model proposed by Graizer and Kalkan (2015). The obtained data were used as scenario earthquakes in SPT and V_s-based liquefaction analyses. Ground motion prediction equation (GMPE) developed by Graizer and Kalkan (2015) is as follows;

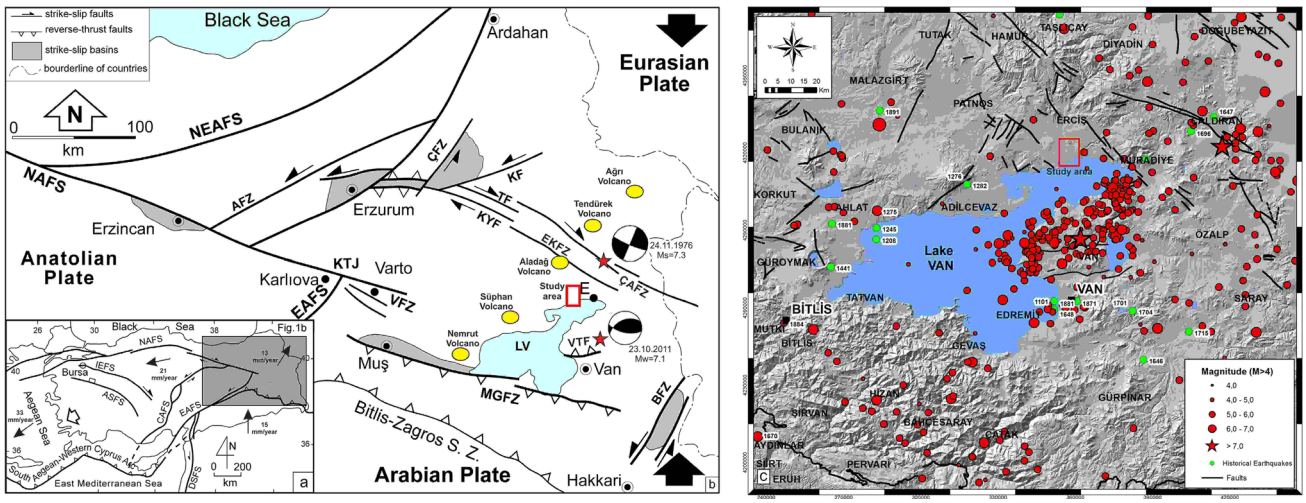

Fig. 4 **a** Tectonic map of Turkey. **b** Simplified tectonic map of Eastern Anatolia (*AFZ* Aşkale fault zone, *BFZ* Başkale fault zone, *ÇFZ* Çobandede fault zone, *ÇAFZ* Çaldıran fault zone, *EAFS* East Anatolian fault zone, *EKFZ* Erciş–Kocapınar fault zone, *NAFS* North Anatolian fault zone, *KF* Kağızman fault zone, *MGFZ* Muş–Gevaş thrust to reverse fault zone, *TF* Tutak fault, *VTF* Van thrust fault, VFZ: Varto fault zone) (modified from Koçyiğit, 2013) **c** the distribution of earthquakes ($M > 4.0$) around the Lake Van

$$\ln(Y) = \ln(G_1) + \ln(G_2) + \ln(G_3) + \ln(G_4) + \ln(G_5) + \sigma_{\ln(\mathrm{PGA})}, \tag{2}$$

where $\sigma_{\ln(\mathrm{PGA})}$ is the random variability and Y is the PGA. The formulations of G_1, G_2, G_3, G_4, and G_5 are given,

$$\begin{aligned}
\ln(G_1) &= \ln[(c_1 \cdot \arctan(M + c_2) + c_3) \cdot F] \\
\ln(G_2) &= -0.5 \cdot \ln\left[(1 - R/(c_4.M + c_5))^2 \right. \\
&\quad \left. + 4.(c_6 \cdot \cos[c_7 \cdot (M + c_8)] + c_9)^2 \cdot (R/(c_4 \cdot M + c_5))\right] \\
\ln(G_3) &= -c_{10} \cdot R/Q_0 \ln(G_4) \\
&= b_v \cdot \ln(V_{s30}/V_A) \ln(G_5) \\
&= \ln\left[1 + A_{\mathrm{Bdist}} \cdot A_{\mathrm{Bdepth}}\right] \\
A_{\mathrm{Bdepth}} &= 1.077/\sqrt{\left[1 - (1.5/(B_{\mathrm{depth}} + 0.1))^2\right]^2 + 4 \cdot 0.7^2 \cdot (1.5/(B_{\mathrm{depth}} + 0.1))^2} \\
A_{\mathrm{Bdist}} &= 1/\sqrt{\left[1 - (40/(R + 0.1))^2\right]^2 + 4 \cdot 0.7^2 \cdot (40/(R + 0.1))^2}
\end{aligned} \tag{3}$$

where M is moment magnitude, F is the style of faulting, and R is the nearest distance to fault rupture plane (km). Q_0 is regional quality factor, and B_{depth} basin depth under the site (km). c_{1-10}, b_v and V_A are coefficients. The model established by Graizer and Kalkan (2015) may be employed for the earthquakes with moment magnitudes of 5.0–8.0, distances from 0 to 250 km, spectral periods of 0.01–5 s and average V_s from 200 to 1300 m/s.

SPT-based liquefaction analyses

Liquefaction analyses were carried out according to the cyclic stress approach. The method proposed by Idriss and Boulanger (2006, 2008) and based on SPT was used in the present research. The liquefaction safety factor is explained as the ratio of the CRR that results in liquefaction for a certain cycle number, to the CSR, generated in the soil as a result of earthquake motion.

During the SPT, the blow counts are highly sensitive to the length of rods, hammer energy, sampler type, borehole diameter and overburden stress (Idriss and Boulanger 2008, 2010). Thus, a corrected penetration resistance is obtained using raw SPT data and a number of correction factors as shown in equation,

$$(N1)_{60} = C_N C_E C_R C_B C_S N_m, \tag{4}$$

where C_N, C_E, C_R, C_B, and C_S are the correction parameters whereas N_m is the SPT blow count obtained in situ (Idriss and Boulanger 2008, 2010).

The safety factor (FS) against liquefaction is determined considering the influence of the magnitude scaling factor (MSF). The corrected SPT-$(N_1)_{60}$ values are taken into consideration in the factor of safety analysis as suggested by Youd et al. (2001) and Idriss and Boulanger (2008).

$$\mathrm{FS} = \frac{\mathrm{CRR}}{\mathrm{CSR}}\,\mathrm{MSF}, \tag{5}$$

FS is the ratio of CRR to CSR, which is an indication of the shear resistance of the soil deposit to liquefaction (CRR) under the influence of the maximum shear stress (CSR) generated by an earthquake. Since the Eq. 5 is appropriate for the magnitude 7.5 earthquakes; a MSF developed by Seed and Idriss (1982) for the earthquakes of diverse magnitudes are used in this study. The soils are assumed to be liquefiable if the safety factor ≤ 1; potentially liquefiable between 1 and 1.2 and non-liquefiable if the safety factor > 1.2 (Seed and Idriss 1982).

Table 1 Major Earthquakes ($M \geq 5$) around the Lake Van between 1900 and 2017 (KOERI http://www.koeri.boun.edu.tr/sismo/2/en/)

Date	Latitude	Longitude	Depth (km)	M	Date	Latitude	Longitude	Depth (km)	M
28.04.1903	39.1	42.5	30	6.3	24.11.1976	39.1	44.2	63	5.5
29.01.1907	39.1	42.5	30	5.2	24.11.1976	39.17	43.95	33	5.1
31.03.1907	39.1	42.5	30	5.4	24.11.1976	39.05	44.04	10	7.3
28.09.1908	38	44	30	6	25.11.1976	38.96	44.28	38	5.1
27.01.1913	38.38	42.23	10	5.5	17.01.1977	39.27	43.7	39	5.3
14.02.1915	38.8	42.5	30	5.7	26.05.1977	38.93	44.38	38	5.4
25.07.1924	38	43	30	5.2	03.12.1984	37.94	43.18	55	5
06.09.1924	39.67	42.81	10	5.2	20.04.1988	39.11	44.12	48	5.1
07.05.1930	38	44.5	30	5.2	25.06.1988	38.5	43.07	49	5.3
08.05.1930	38	44.5	30	5.5	03.06.1991	40.04	42.85	28	5
10.05.1930	37.55	44.25	10	5.2	14.02.1995	37.75	42.96	0	5.4
23.05.1930	38	44.5	30	5.4	15.11.2000	38.28	42.94	8	5.2
29.05.1930	38	44.5	30	5.6	01.07.2004	39.63	43.94	10	5.4
09.07.1930	38	44.5	30	5.2	25.01.2005	37.57	43.68	22	5.9
03.08.1930	38.46	44.7	80	5.3	21.01.2007	39.60	42.82	5	5.1
15.03.1932	39.7	44	15	5.5	23.10.2011	38.63	43.08	5	5.9
18.08.1935	39.6	43.1	30	5.3	23.10.2011	38.70	43.29	2.1	5.1
01.05.1936	39.6	43.1	30	5.7	23.10.2011	38.80	43.25	5	5.7
02.05.1936	39.8	43.5	30	5.3	23.10.2011	38.69	43.04	4.4	5.2
18.10.1940	39.6	42.2	15	5.7	23.10.2011	38.81	43.44	5	5.6
10.09.1941	39.45	43.32	20	5.9	23.10.2011	38.75	43.59	9	5.1
15.01.1945	38.4	44.2	32	5.3	23.10.2011	38.72	43.41	5	7.1
29.07.1945	38	43	30	5.2	24.10.2011	38.73	43.28	5	5
20.11.1945	38.63	43.33	10	5.4	25.10.2011	38.72	43.56	5.2	5.6
03.10.1946	39.5	44.12	50	5.2	27.10.2011	37.20	44.08	10	5.4
19.04.1947	37.8	43.31	40	5.3	29.10.2011	38.89	43.55	10	5.1
04.09.1962	39.96	44.13	40	5.5	08.11.2011	38.72	43.08	6	5.4
27.04.1966	38.14	42.52	28	5.2	09.11.2011	38.42	43.21	6	5.6
02.05.1966	38.1	42.5	50	5	14.11.2011	38.69	43.16	8	5.3
17.05.1967	38.69	44.29	54	5	18.11.2011	38.82	43.83	5	5
29.04.1968	39.24	44.23	17	5.6	30.11.2011	38.47	43.43	4.1	5
11.06.1968	38.15	42.85	53	5.1	26.03.2012	39.16	42.32	5	5
16.07.1972	38.23	43.86	46	5	14.06.2012	37.24	42.42	5	5.5
24.11.1976	39.08	44.13	55	5	05.08.2012	37.41	42.95	8.1	5.4
24.11.1976	39	44.19	62	5					

The liquefaction resistance of soils is represented by the CRR following some essential corrections. The CRR of a soil is affected by the duration time of earthquake as well as the effective overburden stress which is expressed by a K_σ factor. The K_σ is commonly small for shallow ground conditions (Idriss and Boulanger 2008, 2010).

CRR is required to determine the liquefaction safety factor and is calculated as a function of SPT values (Seed and Idriss 1982; Seed et al. 1983; Idriss and Boulanger 2008). Idriss and Boulanger (2008, 2010) expressed the subsequent formula for the determination of CRR, corrected for overburden pressure and magnitude.

$$\mathrm{CRR}_{\sigma=1} = \exp\left(\left(\frac{(N_1)_{60\mathrm{cs}}}{14.1}\right) + \left(\frac{(N_1)_{60\mathrm{cs}}}{126}\right)^2 - \left(\frac{(N_1)_{60\mathrm{cs}}}{23.6}\right)^3 + \left(\frac{(N_1)_{60\mathrm{cs}}}{25.4}\right)^4 - 2.8\right)$$
$$(N1)_{60\mathrm{cs}} < 37.5\ \mathrm{CRR}_{\sigma=1,M=7.5} = 2 \qquad (N1)_{60\mathrm{cs}} > 37.5\ . \tag{6}$$

The following methods for the calculation of CRR are for $\mathrm{CRR}_{7.5}$ and K_σ correction factors should still be applied.

$$\mathrm{CRR} = \mathrm{CRR}_{7.5}\, K_\sigma \tag{7}$$

Table 2 The utilized data of the geotechnical boreholes within the study area

Borehole no	Coordinate		Depth (m)	Groundwater Level	*Average SPT-N	Borehole no	Coordinate		Depth (m)	Groundwater Level	*Average SPT-N	Borehole no	Coordinate		Depth (m)	Groundwater level	*Average SPT-N
	X	*Y*					*X*	*Y*					*X*	*Y*			
ES-1	357838	4321511	15	9	32	ES-56	358498	4316294	24	2.5	20	ES-111	354458	4319433	20	1	34
ES-2	357826	4321522	10	9	33	ES-57	358429	4316189	24	2.5	24	ES-112	354874	4318973	35	0.5	49
ES-3	358992	4320777	16	5	36	ES-58	358532	4316223	27	2	28	ES-113	355303	4319146	20	0.7	16
ES-4	359014	4320764	15	5	40	ES-59	358430	4316130	27	2	28	ES-114	355300	4319447	25	1	37
ES-5	359029	4320754	15	5	40	ES-60	358354	4316255	20	1.5	31	ES-115	354962	4322970	30	1	43
ES-6	359059	4320749	15	5	40	ES-61	357188	4319984	15	4.5	46	ES-116	354796	4319557	30	1	19
ES-7	358954	4320732	20	4.5	46	ES-62	357145	4320071	15	4.5	48	ES-117	356980	4320512	20	5	21
ES-8	358967	4320752	17	4.5	44	ES-63	355267	4321835	15	4.5	43	ES-118	356980	4320471	20	5	21
ES-9	358985	4320775	20	4.5	40	ES-64	355297	4321846	15	4.5	53	ES-119	357015	4320509	20	5	26
ES-10	358969	4320717	18	4.7	37	ES-65	359367	4321371	15	2	37	ES-120	359316	4321752	20	10	25
ES-11	358985	4320738	19	4.7	44	ES-66	359394	4321364	15	2	38	ES-121	358931	4321831	25	8	19
ES-12	359003	4320760	20	5	46	ES-67	355779	4324017	15	2	47	ES-122	358350	4321809	20	8	35
ES-13	358992	4320702	19	5	45	ES-68	356419	4325453	15	2.5	46	ES-123	357826	4321823	25	8	18
ES-14	359006	4320722	20	4.7	44	ES-69	357014	4318726	15	4	31	ES-124	357315	4321804	20	3	22
ES-15	359018	4320747	18	5	42	ES-70	353901	4318353	15	4.5	35	ES-125	356833	4321555	25	10	20
ES-16	359009	4320692	18	5	44	ES-71	353925	4318379	15	4.5	37	ES-126	357348	4321207	25	2	18
ES-17	359021	4320713	19	5	44	ES-72	357191	4321344	15	4	29	ES-127	357827	4321115	20	2	21
ES-18	359036	4320737	18	5	42	ES-73	357170	4321320	15	4	31	ES-128	358396	4321116	22	8	30
ES-19	359025	4320683	20	5	44	ES-74	359374	4321294	10	8.5	49	ES-129	358946	4321140	20	8	24
ES-20	359042	4320703	19	5	41	ES-75	358801	4320760	10	9	49	ES-130	359472	4321121	15	10	22
ES-21	357020	4320555	15	4.5	42	ES-76	358178	4317074	40	1	28	ES-131	359538	4320512	25	10	28
ES-22	357099	4320532	15	4.5	41	ES-77	358051	4317219	20	1.5	27	ES-132	358984	4320520	25	7	19
ES-23	357079	4320608	10	4.5	40	ES-78	357808	4317454	20	0.8	29	ES-133	358427	4320486	30	7	35
ES-24	359376	4321288	10	9	41	ES-79	359702	4317488	20	0.8	18	ES-134	357865	4320478	25	6	18
ES-25	359406	4321313	10	9	44	ES-80	359940	4317906	20	0.2	18	ES-135	357278	4320522	20	3	16
ES-26	357928	4321091	15	4.5	38	ES-81	360781	4317956	20	0.8	24	ES-136	356704	4320663	20	6	15
ES-27	357910	4321092	10	4.5	34	ES-82	359872	4318550	20	2.2	22	ES-137	356795	4319798	20	11	22
ES-28	359096	4320136	10	2.5	39	ES-83	360527	4318194	40	2	25	ES-138	357317	4319777	20	3.5	21
ES-29	359082	4320147	10	2.5	42	ES-84	353917	4324531	30	0.5	45	ES-139	357912	4319726	20	3	21
ES-30	355460	4322150	10	9	54	ES-85	354573	4324427	20	1	38	ES-140	358420	4319727	25	1.5	21
ES-31	355468	4322168	10	9	49	ES-86	354969	4324036	30	1	32	ES-141	358970	4319757	35	0.5	21
ES-32	360084	4320111	15	11	43	ES-87	354670	4323997	20	0.5	46	ES-142	359508	4319756	20	6	21
ES-33	360064	4320151	11	11	37	ES-88	354023	4323932	20	0.5	44	ES-143	357019	4318647	20	4	21
ES-34	358058	4321236	15	3	50	ES-89	354190	4323523	20	0.7	50	ES-144	360580	4319072	20	10	21

Table 2 continued

Borehole no	Coordinate		Depth (m)	Groundwater Level	*Average SPT-N	Borehole no	Coordinate		Depth (m)	Groundwater Level	*Average SPT-N	Borehole no	Coordinate		Depth (m)	Groundwater level	*Average SPT-N
	X	*Y*					*X*	*Y*					*X*	*Y*			
ES-35	358047	4321239	15	3	50	ES-90	354812	4323548	20	0.5	46	ES-145	360051	4319213	25	4	21
ES-36	356669	4321287	20	6	22	ES-91	354983	4323306	25	1	46	ES-146	359545	4319074	20	1	21
ES-37	356688	4321280	20	7.5	24	ES-92	354559	4323387	20	1	48	ES-147	358993	4319210	30	2	16
ES-38	356714	4321278	20	7.5	27	ES-93	353875	4323299	20	1	39	ES-148	358356	4319044	20	1	19
ES-39	356723	4321301	20	10.5	20	ES-94	353719	4322862	30	1	42	ES-149	357885	4319174	20	1	16
ES-40	356667	4321305	20	10.5	21	ES-95	354339	4322794	20	0.5	48	ES-150	357603	4318769	20	1	16
ES-41	356718	4321362	20	10	20	ES-96	354721	4322775	20	1	50	ES-151	357392	4318330	20	1	31
ES-42	356756	4321341	20	10	22	ES-97	355126	4322607	20	1	23	ES-152	357865	4318298	25	2	18
ES-43	356757	4321372	20	10	22	ES-98	354573	4322167	23	1	38	ES-153	358492	4318374	30	2	17
ES-44	356721	4321371	20	7.5	26	ES-99	354018	4322284	20	1	33	ES-154	358956	4318376	35	1.5	30
ES-45	359941	4318919	20	2.5	37	ES-100	353523	4322211	20	1	39	ES-155	359515	4318468	20	4	18
ES-46	359946	4318889	20	2.5	43	ES-101	353914	4321701	20	1	32	ES-156	360127	4318645	20	1	20
ES-47	359972	4318891	20	2.5	45	ES-102	354647	4321637	20	1	41	ES-157	360560	4318641	20	8	36
ES-48	359957	4318926	20	2.5	37	ES-103	354937	4321945	20	1	16	ES-158	359586	4317703	20	1	15
ES-49	357169	4321219	20	3	64	ES-104	355029	4321138	24	1	21	ES-159	358818	4317838	20	1.5	17
ES-50	357201	4321200	20	3	64	ES-105	354567	4321032	30	1	34	ES-160	358426	4317796	20	1	16
ES-51	357211	4321216	20	3	64	ES-106	354200	4321020	20	1	34	ES-161	357871	4317693	20	1	18
ES-52	357178	4321232	20	3	64	ES-107	354147	4320567	20	1.5	43	ES-162	357414	4317813	25	1	18
ES-53	357192	4321214	20	3	64	ES-108	354824	4320202	20	1	20	ES-163	358457	4317124	20	1	20
ES-54	358372	4316353	24	3.5	24	ES-109	354589	4319896	20	1	44	ES-164	358931	4317107	20	1	19
ES-55	358409	4316261	24	3.5	21	ES-110	354037	4319947	20	1	48	ES-165	359309	4317398	25	4	21

*Average of all tests in borehole

Table 3 Seismic measurement points in Erciş settlement area

Measurement point	Coordinates		V_s	$V_{s_{30}}$	Measurement point	Coordinates		V_s	$V_{s_{30}}$
	X	*Y*				*X*	*Y*		
JF-1	358834	4321780	257	303	JF-12	358403	4319327	210	266
JF-2	357845	4320814	226	261	JF-13	358589	4320226	228	289
JF-3	358412	4321020	235	284	JF-14	357419	4321976	249	270
JF-4	356938	4321736	224	254	JF-15	359824	4319987	232	264
JF-5	354377	4321624	251	263	JF-16	360328	4318263	210	250
JF-6	353979	4323405	245	278	JF-17	358353	4316416	184	201
JF-7	354213	4320100	250	281	JF-18	357059	4320320	234	275
JF-8	354174	4318355	234	265	JF-19	357154	4321295	248	298
JF-9	355755	4319970	213	268	JF-20	359992	4319155	210	275
JF-10	359625	4317561	210	243	JF-21	358840	4320901	247	291
JF-11	356741	4317401	221	274					

*The V_s value beneath the groundwater level is used in liquefaction analysis

Table 4 Scenario earthquake parameters used in liquefaction analyses

	Earthquake date	M_s	M_w	R (km)	a_{max} (g)
Erciş fault	1941	5.9	6	11	0.53
Çaldıran fault	1976	7.3	7.1	32	0.28
Van fault	2011	–	7.1	38	0.29

Several expressions using different correction factors have been proposed by various researchers. The most recent one is the work by Idriss and Boulanger (2008). It suggests that the value of K_σ should be less than 1.0 for loose and shallow sediments, and greater than 1.0 for tight grounds (Seed and Harder 1990). Idriss and Boulanger (2006) suggest the following relation for the K_σ and C_σ correction factors.

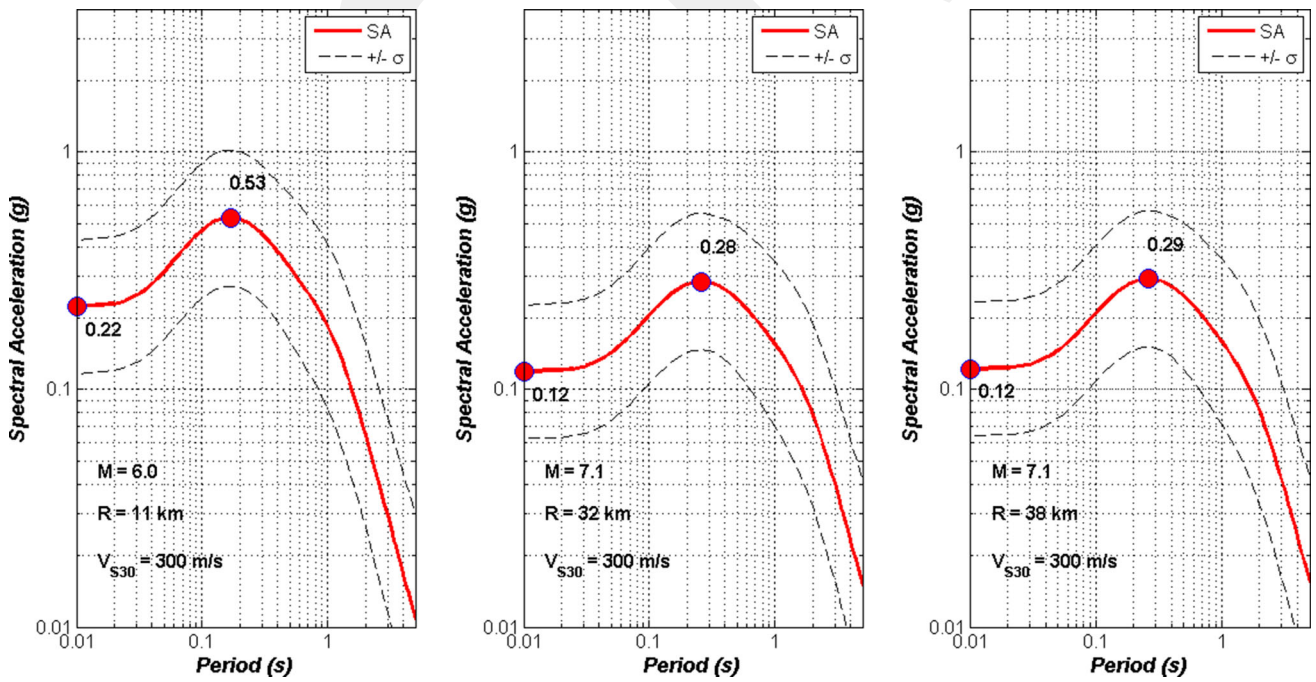

Fig. 5 Peak ground accelerations of Erciş, Çaldıran and Van faults that may affect the study area

$$K_\sigma = 1 - C_\sigma \ln\left(\frac{\sigma'_{vo}}{P_a}\right)$$
$$C_\sigma = \frac{1}{18.9 - 2.55\sqrt{(N1)_{60}}} \quad (8)$$

Idriss and Boulanger (2008, 2010) introduced a new and up-to-date analytical approach to cyclic resistance ratio by creating a large database of liquefaction analyses. Details of this approach are listed below.

$$(N1)_{60CS} = (N1)_{60} + \Delta(N1)_{60CS}$$
$$\Delta(N1)_{60CS} = \exp\left[1.63 + \left(\frac{9.7}{FC + 0.01}\right) - \left(\frac{15.7}{FC + 0.01}\right)^2\right] \quad (9)$$

$$CRR_{7.5} = \exp\left[\frac{(N1)_{60CS}}{14.1} + \left(\frac{(N1)_{60CS}}{126}\right)^2 - \left(\frac{(N1)_{60CS}}{23.6}\right)^3 + \left(\frac{(N1)_{60CS}}{23.6}\right)^4 - 2.8\right]. \quad (10)$$

The CSR under earthquake loads is usually explained as a characteristic rate corresponding to 65% of the maximum cyclic shear stress at a certain depth, z. The CSR is calculated by an equation that considers acceleration, total and effective stresses at various depths, non-rigidity of the deposit, and several assumptions. Seed and Idriss (1971) presented an equation for the calculation of CSR as follows.

$$CSR = \frac{\tau_{av}}{\sigma^t_{vo}} = 0.65\left(\frac{a_{max}}{g}\right)\left(\frac{\sigma_{vo}}{\sigma^t_{vo}}\right) r_d \quad (11)$$

where τ_{av} is the mean cyclic shear stress triggered by earthquake and is accepted to be 65% of the maximum induced stress, g is the acceleration of gravity, a_{max} is the peak ground acceleration (g), σ_{v0} and σ'_{v0} are total and effective stresses at depth z, respectively, and r_d is a stress reduction coefficient.

MSF and reduction factor (r_d) were determined by means of the formulations suggested by Golesorkhi (1989) and Idriss (1999), respectively.

$$Ln(r_d) = \alpha(z) + \beta(z)M_w$$
$$\alpha(z) = -1.012 - 1.126\sin\left(\left(\frac{z}{11.73}\right) + 5.133\right)$$
$$\beta(z) = 0.106 + 0.118\sin\left(\left(\frac{z}{11.28}\right) + 5.142\right), \quad (12)$$

$$MSF = 6.9\exp\left(\frac{-M_w}{4}\right) - 0.058 \qquad M_w > 5.2 \quad (13)$$

where; M_w is the earthquake moment magnitude, z is the depth (m).

LPI and LSI calculations

The LPI method was first introduced by Iwasaki et al. (1978, 1982). LPI depends upon the thickness, depth and liquefaction safety factor of the liquefiable and non-liquefiable layers. LPI provides values for evaluating the liquefaction potentials of liquefiable layers. The equation of LPI is presented in Eq. (14).

$$LPI = \int_0^z F(z)W(z)dz \quad (14)$$

$$W(z) = 10 - 0.5z \qquad z < 20 \text{ m}, \quad (15)$$

where $F(z)$ is the liquefaction safety factor that points out the degree of severity whereas $W(z)$ signifies the depth-based weighting factor. Severity factor [$F(z)$] is designated by the quantitative FS (Sonmez 2003) as follows:

$$F(z) = \begin{cases} FS \le 0.95 & F(z) = 1 - FS \\ 0.95 < FS < 1.2 & F(z) = 2.106\, e^{-18.427\,FS} \\ FS \ge 1.2 & \text{non - liquefaction} \end{cases}. \quad (16)$$

In a sequence with different ground levels, the LPI value is calculated separately for each level. The total LPI value found for each soil level is the sum of the LPI values of the other levels above this level. The total LPI value, in other words the liquefaction potential index of the investigated location specifies the liquefaction risk of the ground (Table 5) (Iwasaki et al. 1982).

The LSI approach has quite different boundary values compared to the LPI method. The maximum value of liquefaction is assumed to be 1.411 in this method (Sonmez and Gokceoglu 2005). According to Sonmez and Gokceoglu (2005), the equation required for the calculation of LSI is presented below.

$$LSI = \int_0^x P(L)W(z)dz \quad (17)$$

The liquefaction probability (P_L) given in the above equation is calculated as follows.

Table 5 Degrees of LPI (Iwasaki et al. 1982)

Liquefaction potential index (LPI)	Liquefaction potential
0	Very low liquefiable
0 < LPI ≤ 5	Low liquefiable
5 < LPI ≤ 15	High liquefiable
15 > LPI	Very high liquefiable

$$P_L = \frac{1}{1+(F_L/0.96)^{4.5}} \quad FL \le 1.411$$
$$P_L(z) = 0 \quad FL > 1.411 \tag{18}$$

On the other hand, $W_{(z)}$ is calculated as in the LPI method. Liquefaction potential classes for the LSI method are given in Table 6.

V_s-based liquefaction analyses

In this study, seismic wave velocity was revealed using seismic refraction and Multichannel Analysis of Surface Waves (MASW) techniques developed by Park et al. (1999). The seismic data can be gathered by this technique and the V_s of soil deposits can be determined using multichannel receivers (Foti 2000; Dikmen et al. 2010a, b). Active source seismograph (12 channels) and 4.5 Hz geophones were employed to acquire data from 21 recording locations in Erciş. Geophone ranges were 3 m, sampling range was 1 ms, as well as record lengths were selected to be 2 s during measurements.

In addition, the V_s values were also calculated for each borehole location depending on the SPT values using the Eq. 19 proposed by Akın et al. (2011) considering the SPT blow counts (N) and depth (z).

$$V_s = 121.75\, N^{-0.101}\, z^{0.216} \quad r = 0.94. \tag{19}$$

In the V_s-based liquefaction analyses, liquefaction potential is determined using acceleration with V_s (Dobry et al. 1981a). The liquefaction potential is defined to be high if the acceleration experienced during an earthquake is greater than 60% of the acceleration that the earth can withstand without being subjected to deformation.

The factor of safety F_a account for the threshold acceleration criteria is as follows:

$$F_a = 1.6\left(\frac{a_t}{a_{max}}\right) \tag{20}$$

where F_a is the safety factor in threshold acceleration criteria, a_t is the threshold acceleration required to start liquefaction, a_{max} is peak ground acceleration of the earthquake. From calculated F_a values obtained using the above mentioned equation, $F_a < 1$ is considered as high liquefaction potential and liquefaction potential is classified as low when $F_a \ge 1$ (Dobry et al. 1981a).

For the calculation of the threshold acceleration value, $\gamma t = 0.0001$ is adopted and the following formula is used by taking into account the corresponding G/G_{max} value as 0.8 (Hardin and Drnevich 1972).

$$\left(\frac{a_t}{g}\right) = \frac{\left[\gamma t \left(\frac{G}{G_{max}}\right) t\, V_s^2\right]}{g\, z\, r_d}$$
$$r_d = 1 - 0.015\, z, \tag{21}$$

where, G_{max} refers to shear modulus, γ is the density of soil, g is the gravity and z is the depth (m).

Andrus and Stokoe (1997, 2000), Uyanık (2002), Uyanık and Taktak (2009) and Uyanik et al. (2013a) suggested several V_s-based liquefaction analyses. FS is generally used for the determination of liquefaction potential using both SPT and V_s data. Seed and Idriss (1971), Uyanık and Taktak (2009) and Uyanik et al. (2013a) formulated the following equation for the calculation of safety factor.

$$FS_{V_s} = \frac{CRR_{V_s}}{CSR_{V_s}} = \frac{SRR}{SSR}. \tag{22}$$

Shear resistance ratio (SRR) is determined as a function of V_s. The SRR and corrected V_s were formulated by Andrus and Stokoe (1997, 2000), Youd et al. (2001), Uyanık (2006) and Uyanık and Taktak (2009).

$$SRR = \left[a\left(\frac{Vs_c}{100}\right)^2 + b\left(\frac{1}{Vs_{max} - Vs_c} - \frac{1}{Vs_{max}}\right)\right] MSF \tag{23}$$

$$V_{s_{max}} = 250 \text{ m/s} \quad FC \le \%5$$
$$V_{s_{max}} = 250 - (FC - 5) \text{ m/s} \quad \%5 < FC < \%35 \tag{24}$$
$$V_{s_{max}} = 220 \text{ m/s} \quad FC \ge \%35,$$

where V_{s_c} is the corrected V_s; $V_{s_{max}}$ is the upper limit of the V_{s_c} and FC is fine content of the soil (Uyanık and Taktak 2009; Uyanik et al. 2013a). MSF is the magnitude scaling factor. a and b are regression coefficients.

Andrus and Stokoe (2000) suggest the values of $V_{s_{max}} = 215$ m/s, $a = 0.022$ and $b = 2.8$ in Eq. 23. Uyanık (2002, 2006) suggests these values as 0.025, 4 and 250 m/s, respectively. Furthermore, Uyanık and Taktak (2009) defined $V_{s_{max}}$ values ranging from 220 to 250 m/s which are related to the fine content of soil.

MSF is a correction coefficient calculated according to earthquake magnitude. The equation developed by Youd et al. (1997) is expressed by the following formula:

Table 6 Degrees of LSI (Sonmez and Gokceoglu 2005)

Liquefaction severity index (LSI)	Liquefaction potential
0	Non-liquefiable
0 < LSI < 15	Very low liquefiable
15 ≤ LSI < 35	Low liquefiable
35 ≤ LSI < 65	Moderate liquefiable
65 ≤ LSI < 85	High liquefiable
85 ≤ LSI < 100	Very high liquefiable

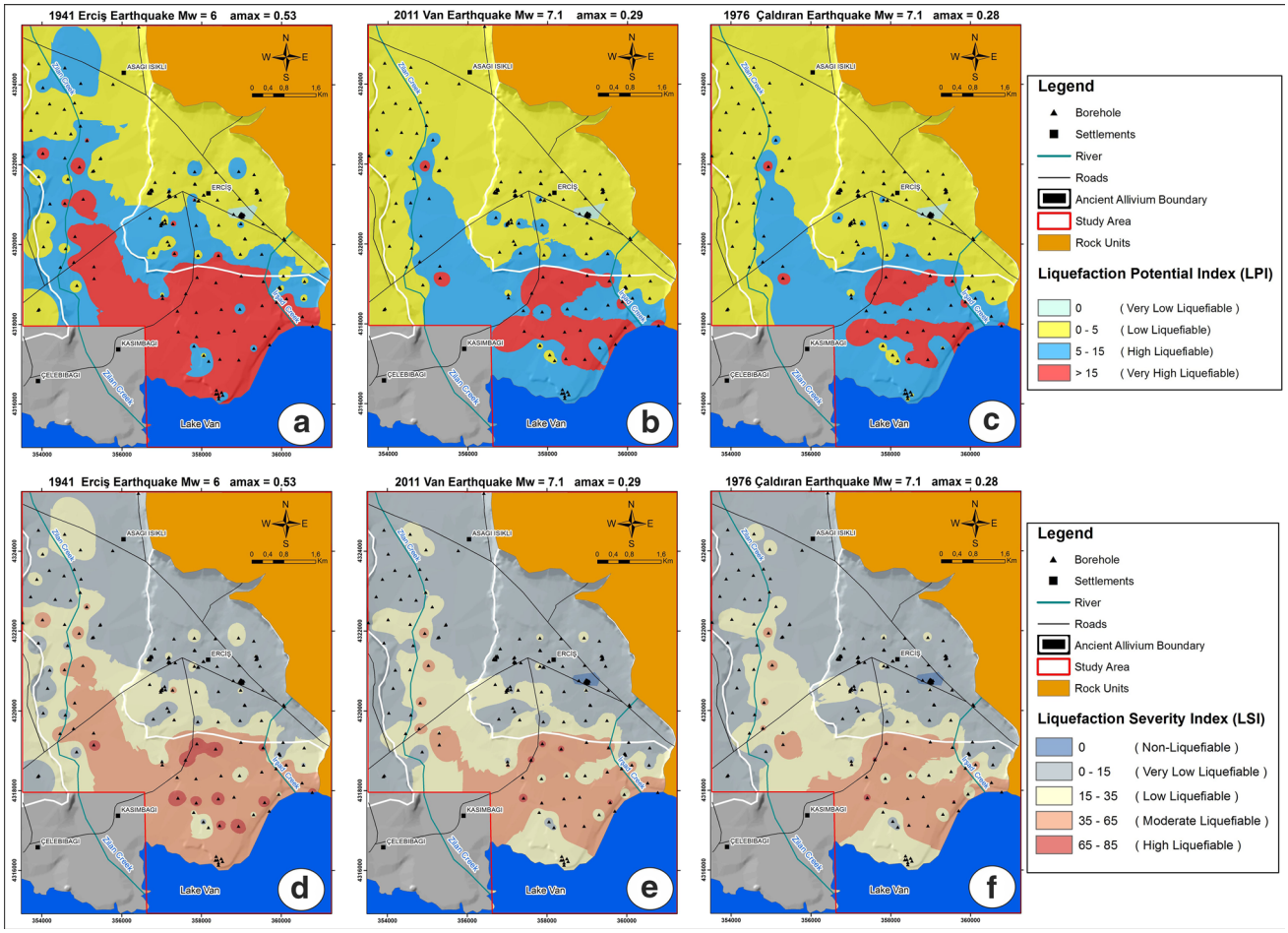

Fig. 6 Liquefaction potential maps of Erciş and its surrounding according to LPI (**a**–**c**) and LSI (**d**–**f**) methods

$$\mathrm{MSF} = \left(\frac{M_w}{7.5}\right)^n \quad (n = -2.56 \;\; M_\mathrm{w} > 7.5 \;\; \text{and} \;\; n = -3.3 \;\; M_\mathrm{w} \leq 7.5 \;\;), \tag{25}$$

where n is exponential constant. Andrus and Stokoe (1997, 2000) propose the following values for the exponential constant (n) obtained depending on the magnitude of the earthquake.

Shear stress ratio (SSR) is the other term required to calculate the factor of safety in terms of liquefaction potential as a function of V_s. CSR and SSR are physically in similar meaning. Nevertheless, the SSR relies on the V_s of the soil deposit and the acceleration as well as the period of the earthquake. The CSR term (in Eq. 11), suggested by Seed and Idriss (1971), is modified as follows using V_s by Uyanık (2002, 2006) and Uyanik et al. (2013a).

$$\mathrm{SSR} = \left(\frac{a_\mathrm{max}}{g}\right)\left(\frac{\sigma_{V_\mathrm{s}}}{\sigma'_{V_\mathrm{s}}}\right) r_\mathrm{d} \tag{26}$$

$$\sigma_{V_\mathrm{s}} = 0.25T\left(\sum_{i=1}^{n} \gamma_i V_{\mathrm{s}_i}\right)$$
$$\sigma'_{V_\mathrm{s}} = \sigma_{V_\mathrm{s}} - u = 0.25T\left(\sum_{i=1}^{n} \gamma_i V_{\mathrm{s}_i} - V_{\mathrm{s}_n}(\gamma_\mathrm{sa} - \gamma_\mathrm{d})\right) \tag{27}$$
$$r_\mathrm{d} = 1 - 0.00765z \quad z \leq 9.15 \text{ m}$$
$$r_\mathrm{d} = 1.174 - 0.0267z \quad 9.15 < z \leq 23 \text{ m}$$
$$r_\mathrm{d} = 0.744 - 0.008z \quad 23 < z \leq 30 \text{ m},$$

where σ'_{V_s} is the effective vertical stress (kN/m^2); σ_{V_s} is the dynamic vertical stress at the investigated depth defined by V_s and earthquake wave period (kN/m^2); a_max is the peak ground acceleration (g), g is the acceleration of gravity, T is the dominant period of the earthquake (s); γ_i is the unit weight of soil layers (kN/m^3); γ_sa saturated unit weight of soil (kN/m^3); γ_d unit weight of unsaturated soil (kN/m^3); V_{s_i} is the V_s velocities of soil unit (m/s); n is the number of layers; z is the depth of layer considered in liquefaction analyses (m) (Uyanık 2002; Uyanık and Taktak 2009; Uyanik et al. 2013a); r_d is a stress reduction coefficient

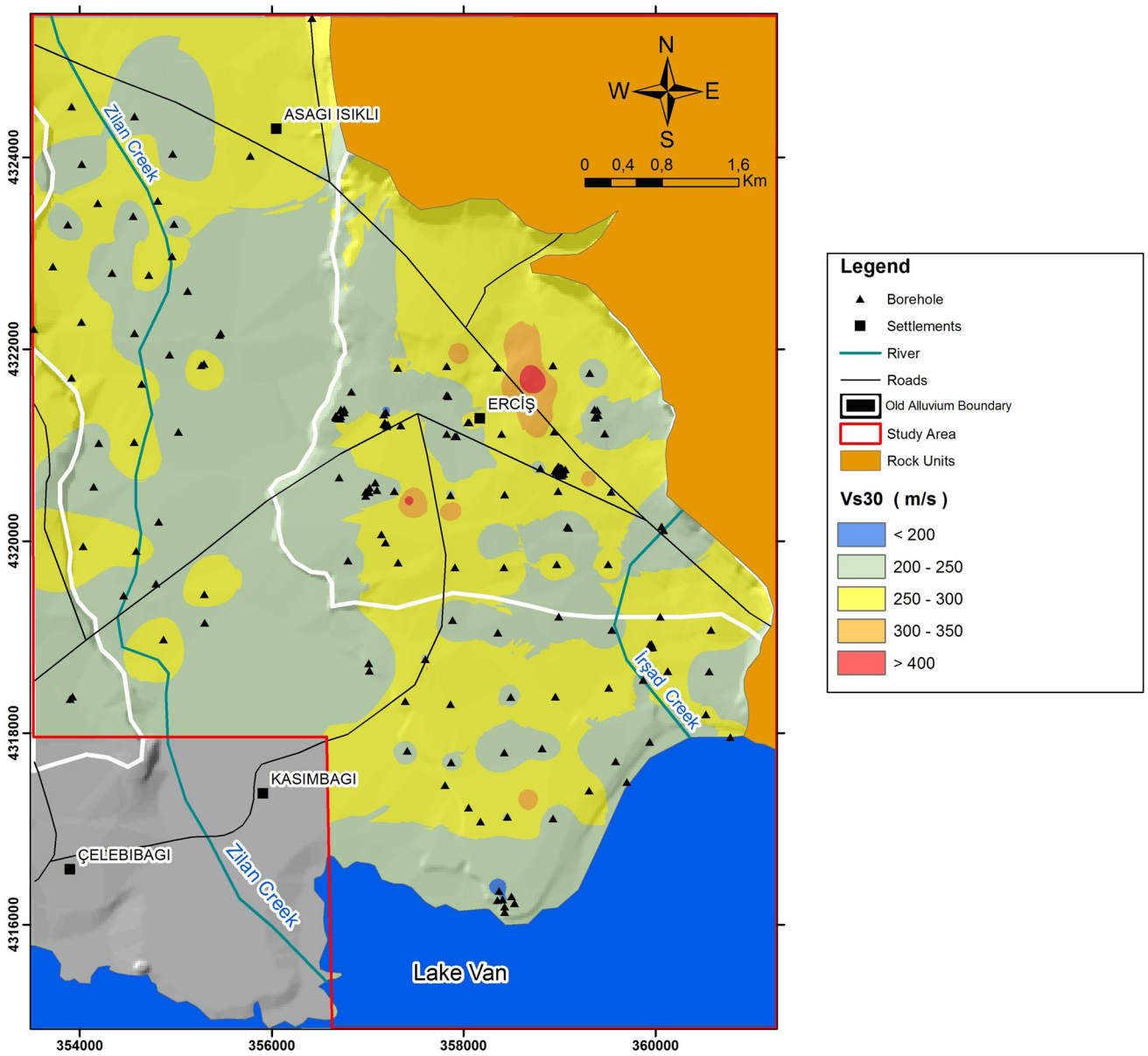

Fig. 7 V_{s30} map of the study area

dependent to depth (Robertson and Wride, 1997; Liao and Whitman, 1986).

To obtain the SSR values from V_s, the V_s values measured in the field should be corrected by a reference overburden stress using the correction factor (Andrus and Stokoe 1997, 2000; Uyanık 2006; Uyanik et al. 2013a).

$$V_{s_c} = V_s \left(\frac{P_a}{\sigma'_{vo}} \right)^{0.25}, \tag{28}$$

where σ'_{V_o} is the effective vertical stress in kPa; V_{s_s} is the corrected V_s (m/s) and P_a is the reference stress which is accepted to be 100 kPa. The SSR is calculated using the earthquake period and V_s values as well as the earthquake acceleration. The SSR value reveals more accurate results when these parameters are used. In this study, the relationships developed by Uyanik et al. (2013a) are used for the calculation of SSR and SRR values.

Results of the liquefaction analyses

Using the SPT, V_s, soil type, groundwater level and earthquake scenarios, the units in the first 20 m in the study area were evaluated in terms of liquefaction potential. As can be seen from the liquefaction potential maps prepared according to the LPI and LSI methods (Fig. 6a–f), the liquefaction potential is determined to be high to very high in all three earthquake scenarios in the coastal sections of

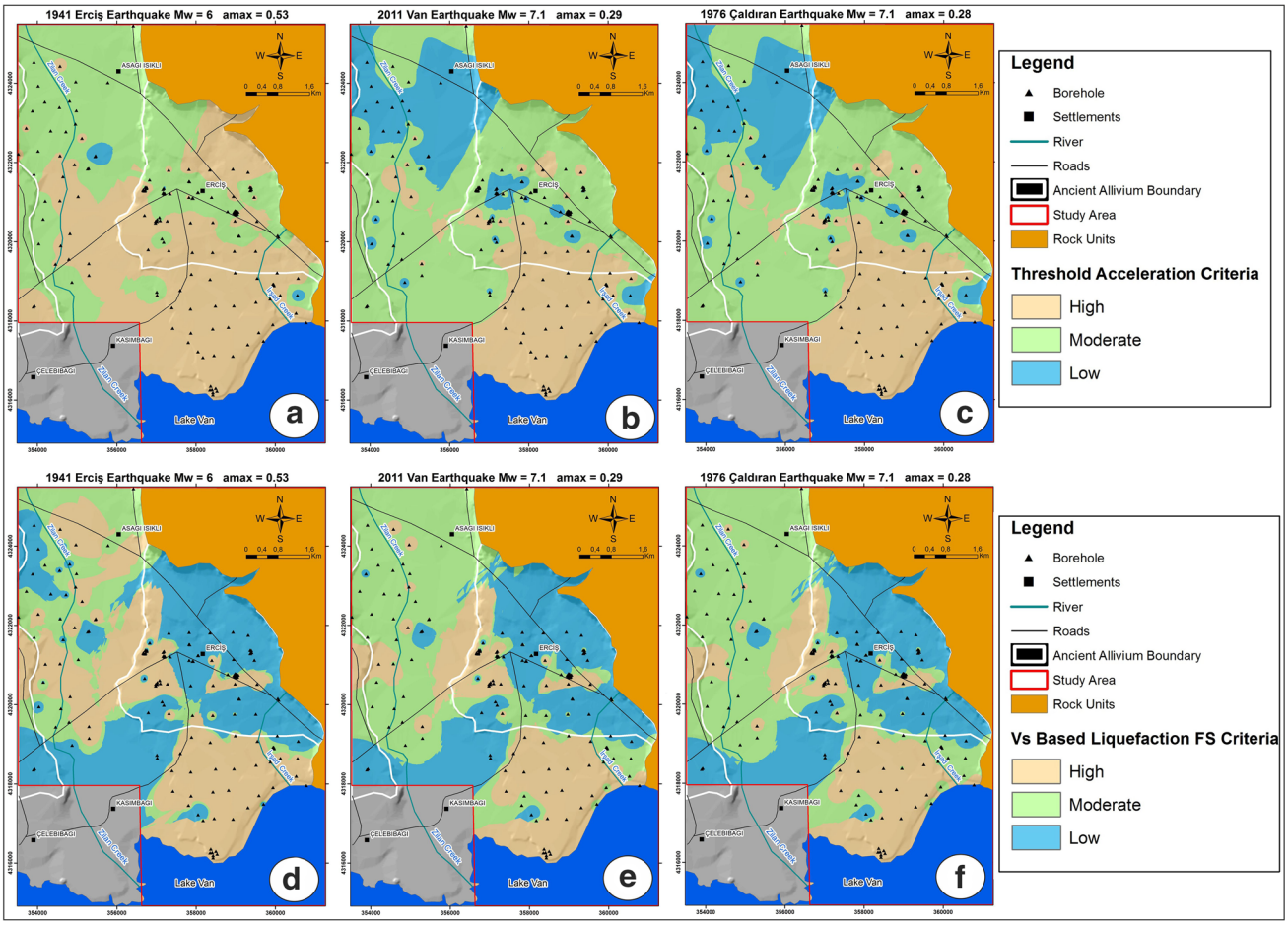

Fig. 8 V_s-based threshold acceleration criteria (**a**–**c**) and safety factor (**d**–**f**) liquefaction potential maps of Erciş and its surrounding

the Lake Van as well as the Zilan Creek in the western part of Erciş and Irşat Creek. However, LPI and LSI values are determined to be low in the western and northern parts of the study area.

$V_{s_{30}}$ value for a depth of 30 m was calculated using seismic methods in the study area, as well (Eq. 28). The $V_{s_{30}}$ velocities in the study area are generally between 200 and 250 m/s in recent alluvial deposits; however, they vary between 250 and 300 m/s in old lacustrine sediments (Fig. 7).

$$V_{s_{30}} = \frac{30}{\sum_{i=1}^{n} \frac{h_i}{V_{s_i}}}. \tag{29}$$

where h_i is the thickness (m) and V_{s_i} is the V_s of the ith layer.

V_s-based threshold acceleration criteria and safety factor were also used to signify the liquefaction potential of the research area (Fig. 8a–f). Similar to the results of LPI and LSI, it was determined that the liquefaction potential is medium to high nearby the Lake Van and in the western region.

Discussion and results

According to four different methodologies (SPT-based LPI and LSI, V_s-based threshold acceleration and safety factor) and three different earthquake scenarios, the liquefaction potential was evaluated for the Erciş district, which suffered the most damage in 2011 Van earthquake. After all these evaluations, it was determined in all four methods that the liquefaction potential of the study area near the coastal parts of the Lake Van and the western part of the study area is higher than the other regions. This indicates that the soil tightness and groundwater level control the liquefaction potential. When three different earthquake scenarios are examined, a high liquefaction potential in Erciş settlement area is determined if Erciş–Kocapınar fault creates an earthquake, which is the closest fault to the study area and there is high-moderate liquefaction potential in the scenarios considering the Çaldıran and Van faults. When all results obtained from those analyses are considered, it is concluded that the LPI and LSI values calculated according to the borehole data and the safety factor liquefaction analyses calculated on the basis of V_s are more

compatible than the threshold acceleration criteria. In addition, it was determined that the location of lateral spreading and sand boils observed in the field after the 23rd October 2011 Van earthquake overlap with the scenario boundaries in this study. Since seismic work can be performed quickly and easily in all types of soil conditions, the use of V_s-based safety factor liquefaction analyses, which reveals consistent results with the SPT-based analyses, is also recommended for the liquefaction assessments.

When liquefaction potential is evaluated according to the methods used in this study, it can be derived that liquefaction type surface deformations may occur after a possible large earthquake in the vicinity of Erciş, especially near the Lake Van from Erciş–Patnos road and in areas close to the rivers. For this reason, considering that the present research is a comprehensive study of the region, liquefaction potential should be evaluated in detail during geotechnical studies carried out for new constructions and soil improvement studies should be executed in areas where liquefaction potential exists.

The raw SPT-N blow counts beneath the groundwater level vary between 4 and 32 when the borehole data and the results of SPT-based liquefaction analyses are considered. Furthermore, it is also concluded that the shallow soils having low shear wave velocity values reveal high liquefaction potential which are compatible with the SPT data. Thus, the use of V_s-based liquefaction analysis in collaboration with the SPT results is quite advantageous to determine the liquefaction potential of a specific site. On the other hand, the SPT data may be misleading where gravelly layers exist within a liquefiable soil whilst the collection of V_s data is rapid and practical.

Acknowledgements This research has been funded by Van Yüzüncü Yıl University the Scientific and Technical Research Council of Turkey (Project No 2014-HIZ-MIM167 and 2015-FBE-YL271). The authors would also like to thank the reviewers for their constructive comments, which enhance the quality of the paper.

References

ABYYHY (1997). Afet Bölgelerinde Yapılacak Yapılar Hakkında Yönetmelik, Aydınoğlu, M. M., Bayındırlık ve İskan Bakanlığı (in Turkish)

Akın, M, Akın MK, Akkaya İ, Özvan A, Şengül MA (2015a) Erciş (Van) Yerleşim Alanındaki Zeminlerin Sıvılaşma Potansiyelinin Değerlendirilmesi, No: 2014-HIZ-MİM167 Yüzüncü Yıl Üniversitesi Bilimsel Araştırma Projeleri Başkanlığı, 46 s (**in Turkish**)

Akın KM, Kramer SL, Topal T (2011) Empirical correlations of shear wave velocity (V_s) and penetration resistance (SPT-N) for different soils in an earthquake-prone area (Erbaa-Turkey). Eng Geol 119(1–2):1–17

Akın M, Özvan A, Akın M, Topal T (2013) Evaluation of liquefaction in Karasu River floodplain after the October 23, 2011, Van (Turkey) earthquake. Nat Hazards 69:1551–1575

Akın M, Akın MK, Akkaya İ, Özvan A, Şengül MA (2015b) Erciş (Van) yerleşim alanındaki zeminlerin sıvılaşma potansiyelinin değerlendirilmesi, Ulusal Mühendislik Jeolojisi Sempozyumu, 3-5 Eylül 2015, KTÜ, Trabzon. s 208-215(**in Turkish**)

Ambraseys NN (2001) Reassessment of earthquakes 1900–1999 in the Eastern Mediterranean and Middle East. Geophys J Int 145:471–485

Andrus RD, Stokoe KH II (2000) Liquefaction resistance of soils from shear-wave velocity. J Geotech Geoenviron Eng (ASCE) 126:1015–1025

Andrus RD and Stokoe II KH (1997) Liquefaction Resistance Based on Shear Wave Velocity. In: NCEER Workshop on Evaluation of Liquefaction Resistance Of Soils, Technical Report NCEER-97-0022, T.L.Youd and I.M. Idriss (Eds.), Held (1996), Salt Lake City, UT, Buffalo, NY, pp 89–128

Aydan Ö, Ulusay R, Kumsar H, Konagai K (2012) Site investigation and engineering evaluation of the Van earthquakes of October 23 and November 9, 2011. Japan Society of Civil Engineers

Aydan Ö, Ulusay R, Kumsar H (2013) Seismic, ground motion and geotechnical characteristics of the 2011 Van-Ercis¸ and Van-Edremit earthquakes of Turkey, and assessment of geotechnical damages. Bull Eng Geol Environ. https://doi.org/10.1007/s10064-013-0526-z

Bozcu M, Uyanık O, Çakmak O, Türker AE (2007) Geotechnical properties of Esen I HEPP Project Field. Süleyman Demirel University. J Nat Appl Sci 11(1):75–83

Bozkurt E (2001) Neotectonics of Turkey-a synthesis. Geodin Acta 14:3–30

Cetin KO, Seed RB, Der Kiureghian A, Tokimatsu K, Harder LF, Kayen RE, Moss RES (2004) Standard penetration test-based probabilistic and deterministic assessment of seismic soil liquefaction potential. J Geotech Geoenviron Eng ASCE 130(12):1314–1340

Dadashpour M, Echeverria-Ciaurri D, Kleppe J, Landro M (2009) Porosity and permeability estimation by integration of production and time-lapse near and far offset seismic data. J Geophys Eng 6:325–344

Dikmen U (2009) Statistical correlations of shear wave velocity and penetration resistance for soils. J Geophys Eng 6:61–72

Dikmen Ü, Arısoy MÖ, Akkaya İ (2010a) Offset and linear spread geometry in MASW method. J Geophy Eng 7:211–222

Dikmen Ü, Başokur AT, Akkaya İ, Arısoy MÖ (2010b) Yüzey dalgalarının çok-kanallı analizi yönteminde uygun atış mesafesinin seçimi. Yerbilimleri 31(1):23–32 **(in Turkish)**

Dobry R, Powell DJ, Yokel FY, Ladd RS (1981a) Geotechnical aspect. Liquefaction potential of saturated sand—the stiffness method. In: Proceeding of the Seventh World Conference on Earthquake Engineering Istanbul, Turkey

Dobry R, Stokoe KHII, Ladd RS, Youd TL (1981b) Liquefaction susceptibility from S-Wave Velocity. In: Proceedings, In Situ Tests to Evaluate Liquefaction Susceptibility, ASCE National Convertion, held 1981, St. Louis, MO

Dobry R, Ladd RS, Yokel FY, Chung RM, Powell D (1982) Prediction of pore water pressure buildup and liquefaction of sands during earthquakes by the cyclic strain method. Building Science Series 138, National Bureau of Standards, US, p 182

Duman ES, Ikizler SB (2014) Assessment of liquefaction potential of Erzincan Province and its vicinity, Turkey. Nat Hazards 73:1863–1887

Foti S (2000) Multistation Methods for Geotechnical Characterization using Surface Waves, Ph.D. Diss., Politecnico di Torino, p 230, Milano

Golesorkhi R (1989) Factors Influencing the Computational Determination of Earthquake-Induced Shear Stresses in Sandy Soils, Ph.D. thesis, University of California at Berkeley, p 395

Graizer V, Kalkan E (2015) Update of the Graizer-Kalkan ground-motion prediction equations for shallow crustal continental earthquakes. USGS Open-File Rep 2015–1009:79

Hardin BO, Drnevich VP (1972) Shear modulus and damping in soils: measurement and parameter effects. J Soil Mech Found Div ASCE. 98(6):603–624

Hasançebi N, Ulusay R (2007) Empirical correlations between shear wave velocity and penetration resistance for ground shaking assessments. Bull Eng Geol Env 66:203–213

Idriss IM (1999) An update to the Seed-Idriss simplified procedure for evaluating liquefaction potential. In: Proceedings, TRB Workshop on New Approaches to Liquefaction, Publication No. FHWARD-99-165, Federal Highway Administration, January

Idriss IM, Boulanger RW (2006) Semi-empirical procedures for evaluating liquefaction potential during earthquakes. Soil Dyn Earthq Eng 26:115–130

Idriss IM, Boulanger RW (2008) Soil liquefaction during earthquakes. Monograph MNO-12, Earthquake Engineering Research Institute, Oakland, p 261

Idriss IM and Boulanger RW (2010) SPT-based Liquefaction Triggering Procedures, Report No. UCD/CGM-10/02, department of Civil & Environmental Engineering College of Engineering University of California, pp 259

Ishihara K (1996) Soil behaviour in earthquake geotechnics. The Oxford Engineering Science Series, Oxford

Iwasaki T, Tokida K, Tatsuko F and Yasuda S (1978) A practical method for assessing soil liquefaction potential based on case studies at various site in Japan. In: 2nd International Conference on Microzonation, San Francisco, pp 885–896

Iwasaki T, Tokida K, Tatsuoka F, Watanabe S, Yasuda S, Sato H (1982) Microzonation for soil liquefaction potential using simplified methods. In: Proceedings of the 3rd international conference on microzonation, Seattle, vol 3, pp 1310–1330

Juang CH, Yuan H, Lee DH, Lin PS (2003) Simplified cone penetration test based method for evaluating liquefaction resistance of soils. J Geotech Geoenviron Eng 129(1):66–80

Kadirioğlu FT, Kartal RF (2016) The new empirical magnitude conversion relations using an improved earthquake catalogue for Turkey and its near vicinity (1900–2012). Turk J of Earth Sc 25:300–310

Karastathis VK, Karmis PN, Draskatos G, Stavrakakis G (2002) Geophysical methods contributing to the testing of concrete dams. Application at the Marathon Dam. J Appl Geophys 50:247–260

Kayen RE, Mitchell JK, Seed RB, Lodge A, Nishio S and Coutinho R (1992) Evaluation of SPT-,CPT-, and shear wave-based methods for liquefaction potential assessment using Loma Prieta data, Fourth Japan-U.S. In: Workshop on Earthquake Resistant Design of Lifeline Facilities and Countermeasures for Soil Liquefaction, Honolulu, Hawaii, Proceedings, Technical Rep. NCEER-92-0019, M. Hamada and T. D. O'Rourke, eds., National Center for Earthquake Engineering Research, Buffalo, NY, 1, pp 177–204

Koçyiğit A (2013) New field and seismic data about the intraplate strike-slip deformation in Van region, East Anatolian plateau, E Turkey. J Asian Earth Sci 62:586–605

Koçyiğit A, Yılmaz A, Adamia S, Kuloshvili S (2001) Neotectonics of East Anotolian Plateau transition from thrusting to strike-slip faulting. Geodin Acta 14:177–195

KOERI (2011) Probabilistic assessment of the seismic hazard for the Lake Van basin, October, 23 2011. www.koeri.boun.edu.tr. Accessed 23 Dec 2011

Kramer SL (1996) Geotechnical earthquake engineering. Prentice-Hall International Series in Civil Engineering and Engineering Mechanics, p 653

Liao SSC, Whitman RV (1986) Overburden correction factors for SPT in sands. J Geotech Eng (ASCE) 112:337–373

MTA (2007) Van İlinin Yer Bilim Verileri, Ankara, s. 69 (**in Turkish**)

Oyan V, Keskin M, Lebedev VA, Chugaev AV, Sharkov EV (2016) Magmatic evolution of the Early Pliocene Etrüsk stratovolcano, Eastern Anatolia collision zone, Turkey. Lithos 256–257:88–108

Özdemir Y, Güleç N (2014) Geological and geochemical evolution of the quaternary Süphan stratovolcano, eastern Anatolia, Turkey: evidence for the lithosphere-asthenosphere interaction in post-collisional volcanism. J Petrol 55:37–62

Özdemir Y, Karaoğlu Ö, Tolluoğlu AÜ, Guleç N (2006) Volcanostratigraphy and petrogenesis of the Nemrutstratovolcano (East Anatolian Plateau): the most recent post-collisional volcanism in Turkey. Chem Geol 226:189–211

Özdemir Y, Akkaya İ, Oyan V, Kelfoun K (2016) A Debris avalanche at Süphan Stratovolcano (Turkey) and implications for hazard evaluation. Bull Volcanol 78(9). https://doi.org/10.1007/s00445-016-1007-6

Özvan A, Şengül MA, Tapan M (2008) Van Gölü havzası Neojen çökellerinin jeoteknik özelliklerine bir bakış: erciş yerleşkesi. Geosound 52:297–310 **(in Turkish)**

Park CB, Miller RD, Xia J (1999) Multichannel analysis of surface waves. Geophysics 64(3):800–808

Pekkan E, Tun M, Guney Y, Mutlu S (2015) Integrated seismic risk analysis using simple weighting method: the case of residential Eskişehir, Turkey. Nat Hazards Earth Syst Sci 15:1123–1133

Robertson PK and Wride CE (1997) Cyclic Liquefaction and Evaluation Based on the SPT and CPT, NCEER Workshop on Evaluation of Liquefaction Resistance of Soils (NCEER-97-0022)

Robertson PK, Wride CE (1998) Evaluating cyclic liquefaction potential using the cone penetration test. Can Geotech J 35(3):442–459

Şaroğlu F, Yilmaz Y (1986) Doğu Anadolu'da Neotektonik Dönemdeki Jeolojik Evrim ve Havza Modelleri. MTA Dergisi 107:73–94 **(Ankara (in Turkish))**

Seed RB and Harder LF (1990) SPT-based analysis of cyclic pore pressure generation and undrained residual strength. In: Froc., HB. Seed Memorial Symp., Hi-Tech Publishing Ltd., vol 2, pp 351–376

Seed HB, Idriss IM (1971) Simplified procedure for evaluating soil liquefaction potential. J Soil Mech Found Div 97:1249–1273

Seed HB, Idriss IM (1982) Ground motions and soil liquefaction during earthquakes. Earthquake Engineering Resarch Institute, Berkeley

Seed HB, Idriss IM, Arango I (1983) Evaluation of liquefaction potential using field performance data. J Geotech Eng ASCE 109:458–482

Selçuk AS (2016) Evaluation of the relative tectonic activity in the eastern Lake Van basin, East Turkey. Geomorphology 270:9–21

Şengör AMC, Kidd WSF (1979) Post-collisional tectonics of the Turkish-Iranian plateau and a comparison with Tibet. Tectonophys. 55:361–376

Şengör AMC, Yılmaz Y (1981) Tethyan evolution of Turkey: a plate tectonic approach. Tectonophysics 75:181–241

Sonmez H (2003) Modification of the liquefaction potential index and liquefaction susceptibility mapping for a liquefactionprone area (Inegol, Turkey). Environ Geol 44:862–871. https://doi.org/10.1007/s00254-003-0831-0

Sonmez H, Gokceoglu C (2005) A liquefaction severity index suggested for engineering practice. Environ Geol 48:81–91

Soupios PM, Papazachos CB, Vargemezis G, Fikos I (2005) Application of Modern Seismic Methods for Geotechnical Site Characterization. In: Πρακτικά του International Workshop in Geoenvironment and Geotechnics 12-14 September 2005, Milos island, Greece, ISBN 960-88153-7-1, σ_λ, pp 163–170

Tezcan SS, Keceli A, Ozdemir Z (2006) Allowable bearing capacity of shallow foundations based on shear wave velocity. J Geotech Geol Eng 24:203–218

Tokimatsu K, Uchida A (1990) Correlation between liquefaction resistance and shear wave velocity. Soils Found 30(2):33–42

Tokimatsu K, Yoshimi Y (1983) Empirical Correlation of Soil Liquefaction Based on SPT N-Value and Fine Content. Soils Found 23(4):56–74

Uyanik O (2010) Compressional and shear-wave velocity measurements in unconsolidated top-soil and comparison of the results. Int J Phys Sci 5(7):1034–1039

Uyanık O (2002) Kayma Dalga Hızına Baglı Potansiyel Sıvılasma Analiz Yöntemi, Doktora Tezi, DEÜ. Fen Bilimleri Enstitüsü, İzmir, 200 s (**in Turkish**)

Uyanık O (2006) Sıvılaşır yada Sıvılaşmaz Zeminlerin Yinelemeli Gerilme Oranına Bir Seçenek, DEÜ Mühendislik Fakültesi Fen ve Mühendislik Dergisi Cilt:8. Sayı 2:79–91 **(in Turkish)**

Uyanık O (2011) The porosity of saturated shallow sediments from seismic compressional and shear wave velocities. J Appl Geophys 73(1):16–24

Uyanık O, Taktak AG (2009) Kayma Dalga Hızı ve Etkin Titresim Periyodundan Sıvılasma Çözümlemesi için Yeni Bir Yöntem. Süleyman Demirel Üniversitesi Fen Bilimleri Enstitüsü Dergisi 13(1):74–81 **(in Turkish)**

Uyanık O, Ulugergerli EU (2008) Quality control of compacted grounds using seismic velocities. Near Surface Geophys 6(5):299–306

Uyanık O, Ekinci B, Uyanık NA (2013a) Liquefaction analysis from seismic velocities and determination of lagoon limits Kumluca/Antalya example. J Appl Geophys 95:90–103

Uyanık O, Türker E, İsmailov T (2006) Sığ Sismik Mikro-Bölgeleme ve Burdur/Türkiye Örneği. Ekologiya ve Su Teserrufatı 1(8):9–15 **(in Turkish)**

Uyanık AN, Uyanık O, Akkurt İ (2013b) Micro-zoning of the natural radioactivity levels and seismic velocities of potential residential areas in volcanic fields: the case of Isparta (Turkey). J Appl Geophys 98:191–204

Watson DF, Philip GM (1985) A refinement of inverse distance weighted interpolation. Geoprocessing 2:315–327

Yi F (2010) Procedure to evaluate liquefaction-induced lateral spreading based on shear wave velocity. In: Fifth International Conference on Recent Advances in Geotechnical Earthquake Engineering and Soil Dynamic, San Diego, California, USA

Youd TL, Idriss IM, Andrus RD, Arango I, Castro G, Christian JT, Dobry R, Finn WDL, Harder Jr LF, Hynes ME, Ishihara K, Koester JP, Liao SSC, Marcuson III WF, Martin GR, Mitchell JK, Moriwaki Y, Power MS, Robertson PK, Seed RB, Stokoe II KH (1997) Summary Report, NCEER Workshop on Evaluation of Liquefaction Resistance of Soils, Technical Report NCEER-97-0022, T.L. Youd and I.M. Idriss, (Eds.), Buffalo, NY, 1-40

Youd TL, Idriss IM, Andrus RD, Arango I, Castro G, Christian JT, Dobry R, Finn WDL, Harder LF Jr, Hynes ME, Ishihara K, Koester JP, Liao SSC, Marcusan WF III, Martin GR, Mitchell JK, Moriwaki Y, Power MS, Robertson PK, Seed RB, Stokoe KH II (2001) Liquefaction resistance of soils: summary report from the 1996 NCEER and 1998 NCEER/NSF Workshops on Evaluation of Liquefaction Resistance of Soils. J Geotech Geoenviron Eng ASCE 127:10